

# Non-Rigid Ultrasound Image Registration Based on Intensity and Local Phase Information

Jonghye Woo · Byung-Woo Hong · Chang-Hong Hu ·  
K. Kirk Shung · C.-C. Jay Kuo · Piotr J. Slomka

Received: 22 January 2008 / Revised: 1 April 2008 / Accepted: 14 April 2008  
© 2008 Springer Science + Business Media, LLC. Manufactured in The United States

**Abstract** A non-rigid ultrasound image registration method is proposed in this work using the intensity as well as the local phase information under a variational framework. One application of this technique is to register two consecutive images in an ultrasound image sequence. Although intensity is the most widely used

feature in traditional ultrasound image registration algorithms, speckle noise and lower image resolution make the registration process difficult. By integrating the intensity and the local phase information, we can find and track the non-rigid transformation of each pixel under diffeomorphism between the source and target images. Experiments using synthetic and cardiac images of *in vivo* mice and human subjects are conducted to demonstrate the advantages of the proposed method.

**Keywords** Ultrasound imaging · Image registration · Local phase · Variational framework

---

This research was partially supported by the Ministry of Knowledge Economy, Korea, under the Home Network Research Center–Information Technology Research Center support program supervised by the Institute of Information Technology Assessment.

---

J. Woo · C.-C. Jay Kuo  
Electrical Engineering, University of Southern California,  
Los Angeles, CA 90089-2564, USA

J. Woo  
e-mail: jonghyew@usc.edu

C.-C. Jay Kuo  
e-mail: cckuo@sipi.usc.edu

B.-W. Hong (✉)  
School of Computer Science and Engineering,  
Chung-Ang University, Seoul 156-756, Korea  
e-mail: hong@cau.ac.kr

C.-H. Hu · K. K. Shung  
Biomedical Engineering, University of Southern California,  
Los Angeles, CA 90089-1451, USA

C.-H. Hu  
e-mail: changhoh@usc.edu

K. K. Shung  
e-mail: kkshung@usc.edu

P. J. Slomka  
Department of Imaging, Cedars-Sinai  
Medical Center, Los Angeles, CA, USA  
e-mail: Piotr.Slomka@cshs.org

## 1 Introduction

Ultrasound imaging has been widely used as a medical imaging modality during last several decades due to its non-invasiveness, safety and economical efficiency [1, 2]. For instance, the use of ultrasound is suitable for fetus imaging and the diagnosis and assessment of arterial and cardiac diseases [3]. Left ventricular contractile function can also be evaluated effectively by echocardiography imaging [4]. However, ultrasound images have a low signal-to-noise (SNR) ratio due to artifacts and attenuation. Furthermore, speckle noise caused by sub-resolution tissue structures is a big foe in analyzing lesions and performing various processes such as segmentation and registration by limiting the detectability of low contrast lesions. Due to these limitations, validation of estimated motion is currently performed in a subjective visual manner.

Registration of ultrasound images can be used in estimating cardiac motion and/or velocities to find

abnormalities in segmental wall motion and analyzing tissue mechanic properties such as quantification of elasticity and contractility of the myocardium [5]. It could be also used for spatial compounding of images to improve image quality and contrast [6]. In general, registration of ultrasound images is a challenging task as compared with that of computed tomography or magnetic resonance imaging due to special properties of ultrasound images, including speckle noise artifacts and low images contrast.

Broadly speaking, registration algorithms can be categorized to two classes: rigid registration using linear transformation (translation, rotation and scaling) and non-rigid registration using nonlinear transformation to compensate for changes in organs or tissue due to the breathing pattern or movement of internal organs [7]. Non-rigid registration using variational minimization and/or various similarity measures is well studied in the context of computer vision. For example, to determine optical flow in temporal images can be viewed as a registration problem [8, 9].

In this work, we propose a novel registration method that exploits both intensity and local phase information by incorporating them in a variational framework and present some preliminary results when this technique is applied to test ultrasound images. The local phase feature is well-suited for ultrasound image registration since it is invariant to image brightness, contrast and noise [10]. We combined this feature with image intensity to register different frames in more accurate manner. To the best of our knowledge, this is the first effort in deriving an energy cost using the intensity and the local phase information under the variational framework to solve the ultrasound image registration problem.

The rest of this paper is organized as follows. Some previous work is reviewed in Section 2. The local phase and its properties are discussed in Section 3. The registration method derived based on the variational framework is presented in Section 4. Experimental results are shown in Section 5. Finally, concluding remarks and future research directions are given in Section 6.

## 2 Review of Previous Work

Several registration methods have been proposed before. They are usually classified into two types: the feature-based approach using extracted image features and the volume-based method using statistical voxel dependencies [11]. Although intensity values contain all available information in images, other derived features may reveal the underlying image structure more

clearly [10]. Thus, we may need to search for additional relevant features and then study how to apply these features jointly for efficient non-rigid ultrasound image registration [7].

Different features have been incorporated to tackle the ultrasound image registration problem. Quite a few registration methods are based on the intensity information in the image registration [12–14] under the assumption that mono-modal images are identical when correctly aligned. An intensity-based deformable registration technique for 3D ultrasound images was presented in [15] under a variational framework. However, this method may not work well since the assumption of gray value constancy may not hold in ultrasound images. For example, it is difficult to detect the heart muscle consistently, thus resulting missing and/or false positives.

Gradient-based methods are conducted based on the assumption that the contrast of a pattern is invariant over time. However, computed gradient values are highly sensitive to noise since the differentiation of gray levels tends to magnify noise, leading to inaccurate results. Intensity and its derivatives were used to generate an attribute vector in [16]. Generally speaking, the gradient-based approach is not suitable for the processing of noisy ultrasound images.

Another class of registration methods is developed based on finding the corresponding landmarks and, furthermore, two images are aligned with approximating thin-plate splines [17]. However, it demands manual selection of landmark points, and finding landmark points is a difficult task especially for ultrasound images.

The local phase feature has been developed by Morrone et al. [18] and has become increasingly popular. Its robustness and accuracy for ultrasound images were studied in [19–21]. The local phase information can provide more local structural information than the intensity feature. We demonstrate in this manuscript that, when the intensity and the local phase information can be combined, they can supplement each other, thereby achieving better registration results.

## 3 Local Phase Computation and Properties

### 3.1 Local Phase and Local Energy

The local phase function provides a qualitative, contrast invariant, local description of an image. It can be interpreted as an amplitude-weighted phase of a windowed (bandpass filtered) Fourier component of a signal [20]. We will show in this section that the local phase serves as an effective feature for ultrasound

image registration. The concept of local phase and local energy were originally developed for analyzing one dimensional signals. The analytic signal is most easily interpreted in terms of Fourier analysis [10].

The analytic signal,  $f_A(x)$ , of a real signal,  $f(x)$ , in the space domain can be written as

$$f_A(x) = f(x) - j f_H(x), \tag{1}$$

where  $f_H(x)$  is the Hilbert transform of  $f(x)$ , defined by

$$f_H(x) = \frac{1}{\pi} \int_{-\infty}^{\infty} \frac{f(\tau) d\tau}{\tau - x} \Leftrightarrow F_H(\omega) = F(\omega) \cdot j \text{sign}(\omega), \tag{2}$$

where  $F(\omega)$  is the Fourier transform of  $f(x)$  and

$$\text{sign}(\omega) = \begin{cases} -1, & \omega < 0, \\ +1, & \omega \geq 0. \end{cases} \tag{3}$$

As given in Eq. 1,  $F_A(\omega)$  is equal to zero at the negative frequency and is twice of the original signal at the positive frequency, which results in an analytic signal given by [22, 23]

$$\begin{aligned} F_A(\omega) &= F(\omega) - j \cdot F_H(\omega) \\ F_A(\omega) &= F(\omega) - j \cdot F(\omega) \cdot j \text{sign}(\omega) \\ F_A(\omega) &= F(\omega) \cdot [1 + \text{sign}(\omega)] \end{aligned} \tag{4}$$

Then, the local phase  $\phi(x)$  and local energy  $A(x)$  of signal  $f(x)$  is defined as

$$\begin{aligned} \phi(x) &= \tan^{-1}(f(x)/f_H(x)), \\ A(x) &= \|f_A(x)\| = \sqrt{f^2(x) + f_H^2(x)}. \end{aligned} \tag{5}$$

However, it is difficult to compute the local phase based on the above definition directly. To extract the proper feature, both time and frequency localization is desired.

In other words, we may apply a window function of bandpass filtering characteristics to  $f(x)$  with an objective to reduce the fine scale noise effect and localize the desired signal. The window function has two properties. First, it should be even and symmetric to maintain the phase information of the original signal. Second, it should have the zero DC value so that steady-state values will not be affected. There are several choices in the design of bandpass filters. We adopt the Difference of Gaussian (DoG) in our work.

### 3.2 Monogenic Signal

It is difficult to extend the Hilbert transform from 1D to 2D directly. For several years it is found that there is no straightforward extension of the Hilbert transform to higher dimensions. Instead, the monogenic signal was proposed in [23] to estimate and extend the phase notion to 2D efficiently. This representation preserves core properties such as isotropic properties of 1D analytic signals and decomposes a signal into the energy and the structure (local phase) features. The even filter is rotationally symmetric (DoG), and the single odd filter used previously is replaced by two odd isotropic filters (vector-valued) in the frequency domain as

$$H_1 = \frac{u}{\sqrt{u^2 + v^2}}, \quad H_2 = \frac{v}{\sqrt{u^2 + v^2}}, \tag{6}$$

where  $u$  and  $v$  are frequency-domain variables. Then, the local phase,  $\phi$ , and local energy can be calculated using a bandpass filtered image  $I_b$  and its filter responses as

$$\begin{aligned} \phi(x, y) &= \tan^{-1} \left( \frac{I_b}{\sqrt{(h_1 * I_b) + (h_2 * I_b)}} \right), \\ E(x, y) &= \sqrt{I^2 + (h_1 * I_b)^2 + (h_2 * I_b)^2}, \end{aligned} \tag{7}$$

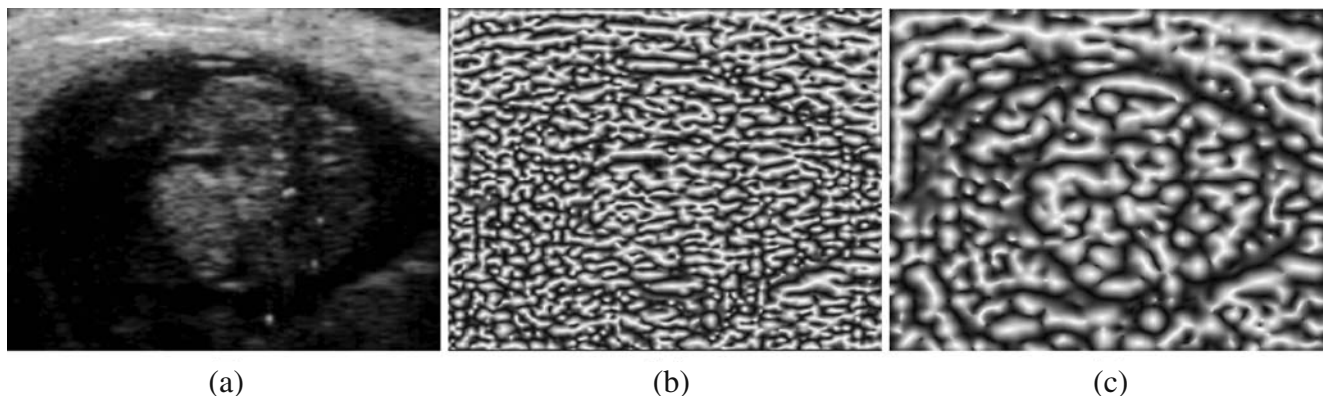


**Figure 1** **a** An exemplary cardiac ultrasound image, and its local phases using two DoG bandpass filters with **b** a small standard deviation ( $\sigma_1 = 2\sqrt{2}, \sigma_2 = 2$ ) and **c** a large standard deviation ( $\sigma_1 = 4\sqrt{2}, \sigma_2 = 4$ ).

where  $*$  denotes the convolution operator. The local phase can be interpreted as a qualitative description of salient regions in images such as edges or ridges. An exemplary cardiac ultrasound image, and its local phases using two DoG bandpass filters with a small and a large standard deviations are shown in Fig. 1. We see from this figure that the local phase provides valuable structure information of the underlying image.

### 4 Registration Method

The problem of ultrasound image registration is equivalent to finding the displacement vector under diffeomorphism between the source and the target images. One application of this technique is to register two consecutive images in an ultrasound image sequence. Then, the source and the target images are the previous and the current image frames, respectively, and the displacement vector denotes the motion field of an image pixel.

#### 4.1 Variational Framework

Before deriving a variational formulation for the registration problem, we provide some intuitive explanations on constraints and assumptions used in this model. The proposed registration method is derived from a variational framework based on the following observations.

The intensity and its derivatives, which are commonly used as features in mono-modal image registration and optical flow estimation, have similar values over two consecutive image frames. The property, called gray value constancy, can be written mathematically as

$$\begin{aligned}
 I(x, y, t) &\approx I(x + u, y + v, t + 1) \\
 \nabla I(x, y, t) &\approx \nabla I(x + u, y + v, t + 1),
 \end{aligned}
 \tag{8}$$

where  $I : \Omega \subset \mathbb{R}^3 \rightarrow \mathbb{R}$  denotes an image sequence,  $(u, v)$  is the local displacement vector of a pixel over two adjacent frames,  $t$  is the frame index number, and  $\nabla = (\partial_x, \partial_y)$  is the 2D spatial gradient vector. The linearized formula of Eq. 8 yields the following optical flow constraint [24]:

$$I_x u + I_y v + I_t = 0, \tag{9}$$

where  $I_x = \partial_x I$  and  $I_y = \partial_y I$ . However, Eq. 9 alone does not carry sufficient and accurate information for ultrasound image registration due to low contrast and low resolution nature of the underlying images. In contrast, as explained in Section 3, the local phase value

is a more accurate feature than the intensity value in ultrasound imaging. It is assumed that local phase values are also similar along their temporal trajectory curves:

$$LP(x, y, t) = LP(x + u, y + v, t + 1), \tag{10}$$

where  $LP$  is the local phase of a given image. The registration problem is however an ill-posed one. That is, the model given in Eqs. 8 and 10 estimates the displacement of a pixel only without taking any neighborhood relation into account. Thus, a piecewise smooth flow is needed for regularization since a problem occurs in the model when the gradient vanishes.

Let  $\mathbf{x} = (x, y)^T$  and  $\mathbf{w}(\mathbf{x}) = \mathbf{w}(x, y) = (u(x, y), v(x, y))^T$ . Then, we can incorporate the intensity and the local phase in the data term as

$$\begin{aligned}
 E_{data}(u, v) = \int_{\Omega} \Psi ( &|S_I(\mathbf{x} + \mathbf{w}(\mathbf{x})) - T_I(\mathbf{x})|^2 \\
 &+ \gamma |S_{LP}(\mathbf{x} + \mathbf{w}(\mathbf{x})) - T_{LP}(\mathbf{x})|^2) d\mathbf{x},
 \end{aligned}
 \tag{11}$$

where  $\gamma$  is a weight, and  $\Psi$  is a quadrature penalizer (e.g.,  $\Psi(s^2) = \sqrt{s^2 + \epsilon^2}$ , which results in modified  $L^1$  norm), and  $S_I, S_{LP}, T_I$  and  $T_{LP}$  are the intensity and the local phase of source image  $S$  and target image  $T$ , respectively.

The smoothness term is derived under the assumption of a piecewise smooth flow field. This can be achieved by penalizing the total variation of the flow field and expressed as

$$E_{smooth}(u, v) = \int_{\Omega} \Psi (|\nabla u|^2 + |\nabla v|^2) d\mathbf{x} \tag{12}$$

with the same  $\Psi$  function as defined above. The total energy functional can be expressed as the weighted sum of the data term and the smoothness term:

$$E(u, v) = E_{data} + \alpha E_{smooth}. \tag{13}$$

By adjusting  $\alpha$ , we can control the balance between the data term and the smoothness term. The smoothness term can prevent overfitting to the data term and produce a piecewise continuous solution.

#### 4.2 Euler–Lagrange Optimization

The energy functional in Eq. 13 can be minimized for the desired gradient descent using the Euler-Lagrange method. With the calculus of variation, the proposed

energy functional satisfies the following Euler–Lagrange equation with respect to  $u$  and  $v$  as

$$\begin{aligned} &\tilde{\Psi}(I_d^2 + \gamma LP_d^2) \cdot (I_d I_x + LP_d LP_x) \\ &\quad - \alpha \operatorname{div}(\tilde{\Psi}(|\nabla u|^2 + |\nabla v|^2)\nabla u) = 0, \\ &\tilde{\Psi}(I_d^2 + \gamma LP_d^2) \cdot (I_d I_y + LP_d LP_y) \\ &\quad - \alpha \operatorname{div}(\tilde{\Psi}(|\nabla u|^2 + |\nabla v|^2)\nabla v) = 0, \end{aligned} \tag{14}$$

where

$$\begin{aligned} I_d &:= S_I(\mathbf{x} + \mathbf{w}) - T_I(\mathbf{x}), \\ LP_d &:= S_{LP}(\mathbf{x} + \mathbf{w}) - T_{LP}(\mathbf{x}), \\ I_x &:= \partial_x S_I(\mathbf{x} + \mathbf{w}), \\ I_y &:= \partial_y S_I(\mathbf{x} + \mathbf{w}), \\ LP_x &:= \partial_x S_{LP}(\mathbf{x} + \mathbf{w}), \\ LP_y &:= \partial_y S_{LP}(\mathbf{x} + \mathbf{w}). \end{aligned} \tag{15}$$

and

$$\tilde{\Psi}(x) = \Psi'(x) = \frac{1}{2\sqrt{x + \varepsilon^2}}$$

and where  $\varepsilon$  is a small number. In our experiment, we choose  $\varepsilon = 0.001$ .

### 4.3 Numerical Approximation

To solve the Euler–lagrange equations in Eq. 14, we adopt an alternating minimization method. That is, we first minimize the energy functional with respect to variable  $u$  with fixed variable  $v$  and, then, minimize the energy functional with respect to variable  $v$  with fixed variable  $u$ . This alternating optimization process can be performed iteratively.

Let us consider the minimization process with respect to variable  $u$ . We define

$$\begin{aligned} F_N(\varepsilon) &= E(u + \varepsilon N, v) \\ &= \int_{\Omega} \Psi(|S_I(x + u + \varepsilon N, y + v) - T_I(x, y)|^2 \\ &\quad + \gamma |S_{LP}(x + u + \varepsilon N, y + v) - T_{LP}(x, y)|^2) d\mathbf{x} \\ &\quad + \alpha \int_{\Omega} \Psi(|\nabla(u + \varepsilon N)|^2 + |\nabla v|^2) d\mathbf{x} \end{aligned} \tag{16}$$

where  $\varepsilon$  is a small parameter. If  $u^*$  is the minimizer, we have  $F_N(0) \leq F_N(\varepsilon), \forall \varepsilon$ . Thus, we have derived the following condition:

$$\left. \frac{dF_N(\varepsilon)}{d\varepsilon} \right|_{u=u^*, \varepsilon=0} = 0. \tag{17}$$

Let

$$F'_N(\varepsilon) = \frac{dF_N(\varepsilon)}{d\varepsilon}.$$

It is straightforward to find that

$$\begin{aligned} F'_N(\varepsilon) &= \int_{\Omega} 2\Psi'(|S_I(x + u, y + v) - T_I(x, y)|^2 \\ &\quad + \gamma |S_{LP}(x + u, y + v) - T_{LP}(x, y)|^2) \\ &\quad \cdot \left[ \frac{\partial S_I(x + u + \varepsilon N, y + v)}{\partial(x + u + \varepsilon N)} \right. \\ &\quad \left. + \gamma \frac{\partial S_{LP}(x + u + \varepsilon N, y + v)}{\partial(x + u + \varepsilon N)} \right] \cdot N d\mathbf{x} \\ &\quad + \alpha \int_{\Omega} 2\Psi'(|\nabla u|^2 + |\nabla v|^2) \\ &\quad \cdot \left[ \left( \frac{\partial u}{\partial x} + \varepsilon \frac{\partial N}{\partial x} \right) \cdot \frac{\partial N}{\partial x} \left( \frac{\partial u}{\partial y} + \varepsilon \frac{\partial N}{\partial y} \right) \cdot \frac{\partial N}{\partial y} \right] d\mathbf{x} \end{aligned} \tag{18}$$

By setting  $\varepsilon = 0$ , we obtain

$$\begin{aligned} F'_N(0) &= \int_{\Omega} 2\Psi'(|S_I(x + u, y + v) - T_I(x, y)|^2 \\ &\quad + \gamma |S_{LP}(x + u, y + v) - T_{LP}(x, y)|^2) \\ &\quad \cdot \left[ \frac{\partial S_I(x + u, y + v)}{\partial(x + u)} \right. \\ &\quad \left. + \gamma \frac{\partial S_{LP}(x + u, y + v)}{\partial(x + u)} \right] \cdot N d\mathbf{x} \\ &\quad + \alpha \int_{\Omega} 2\Psi'(|\nabla u|^2 + |\nabla v|^2) \\ &\quad \cdot \left[ \frac{\partial u}{\partial x} \cdot \frac{\partial N}{\partial x} + \frac{\partial u}{\partial y} \cdot \frac{\partial N}{\partial y} \right] d\mathbf{x} \end{aligned} \tag{19}$$

Then, we can apply integration by parts to the last integral as

$$\int_{\Omega} (\partial_i \cdot u) \cdot v dx = - \int_{\Omega} u(\partial_i v) dx + \int_{\partial\Omega} (u \cdot n_i) \cdot v ds, \tag{20}$$

where  $n_i$  is a component along the normal direction. By setting  $F'_N(0) = 0, \forall N$ , we obtain the Euler-Lagrange equation in  $u$  as

$$\begin{aligned} &\Psi'(|S_I(x + u, y + v) - T_I(x, y)|^2 \\ &\quad + \gamma |S_{LP}(x + u, y + v) - T_{LP}(x, y)|^2) \\ &\quad \cdot \left[ \frac{\partial S_I(x + u, y + v)}{\partial(x + u)} + \gamma \frac{\partial S_{LP}(x + u, y + v)}{\partial(x + u)} \right] \\ &= \alpha \Psi'(|\nabla u|^2 + |\nabla v|^2) \cdot (\Delta u) \end{aligned} \tag{21}$$

The above equation can be put in time-dependent form using the gradient descent as

$$\frac{\partial u}{\partial t} = - \frac{\delta E}{\delta u} = - \left. \frac{dF_N(\varepsilon)}{d\varepsilon} \right|_{\varepsilon=0}, \tag{22}$$

where  $t$  is an artificial time. Then, we have

$$\begin{aligned} \frac{\partial u}{\partial t} = & -\Psi'(|S_I(x+u, y+v) - T_I(x, y)|^2 \\ & + \gamma |S_{LP}(x+u, y+v) - T_{LP}(x, y)|^2) \\ & \cdot \left[ \frac{\partial S_I(x+u, y+v)}{\partial(x+u)} + \gamma \frac{\partial S_{LP}(x+u, y+v)}{\partial(x+u)} \right] \\ & + \alpha \Psi'(|\nabla u|^2 + |\nabla v|^2) \cdot (\Delta u) \end{aligned} \tag{23}$$

We are able to solve Eq. 23 for  $u^*$  numerically. In the numerical implementation, we adopt the following approximation for time differencing:

$$\frac{\partial u}{\partial t} \approx \frac{u^{(n+1)}(i, j) - u^{(n)}(i, j)}{\Delta t}, \tag{24}$$

and the following 5-point approximation for the Laplacian operator:

$$\begin{aligned} \Delta u = & \frac{u(i+1, j) - 2u(i, j) + u(i-1, j)}{h^2} \\ & + \frac{u(i, j+1) - 2u(i, j) + u(i, j-1)}{h^2}. \end{aligned} \tag{25}$$

As a result, we adopt the explicit scheme to solve the above equation with small  $\Delta t$  of the following form:

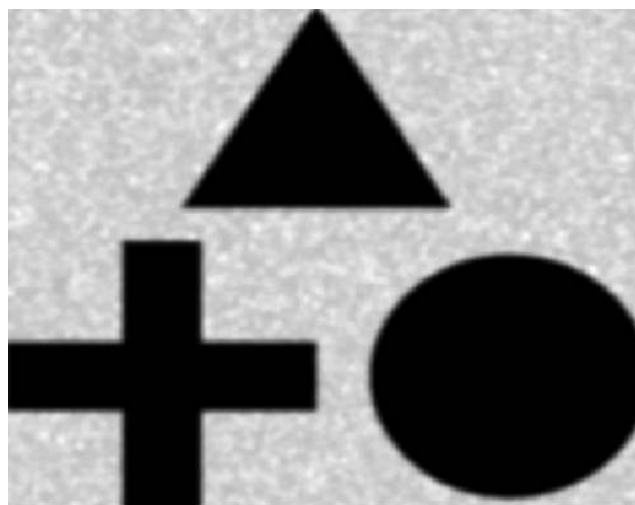
$$\begin{aligned} \frac{u^{(n+1)}(i, j) - u^{(n)}(i, j)}{\Delta t} = & -\Psi'(|S_I(x+u, y+v) - T_I(x, y)|^2 \\ & + \gamma |S_{LP}(x+u, y+v) - T_{LP}(x, y)|^2) \\ & \cdot \left[ \frac{\partial S_I(x+u, y+v)}{\partial(x+u)} \right. \\ & \left. + \gamma \frac{\partial S_{LP}(x+u, y+v)}{\partial(x+u)} \right] \\ & + \alpha \Psi'(|\nabla u|^2 + |\nabla v|^2) \cdot (\Delta u) \end{aligned} \tag{26}$$

Following a similar procedure, the energy functional can be minimized with respect to  $v$ .

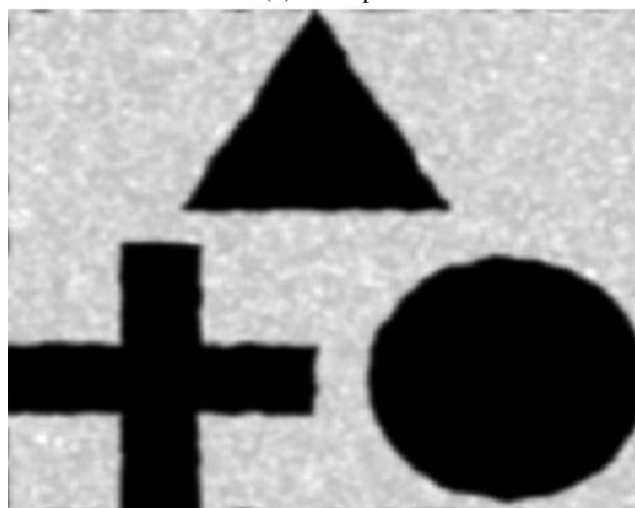
## 5 Experimental Results

### 5.1 Synthetic Images

We begin with some simple yet illustrative examples to demonstrate the efficiency and robustness of the proposed algorithm. Two synthetic images are used in our quantitative validation as shown in Figs. 2a and 3a. Figure 2a consists of simple geometrical shapes while Fig. 3a is the cyst phantom that consists of a collection of point targets, five cyst regions and five highly



(b) Example 1

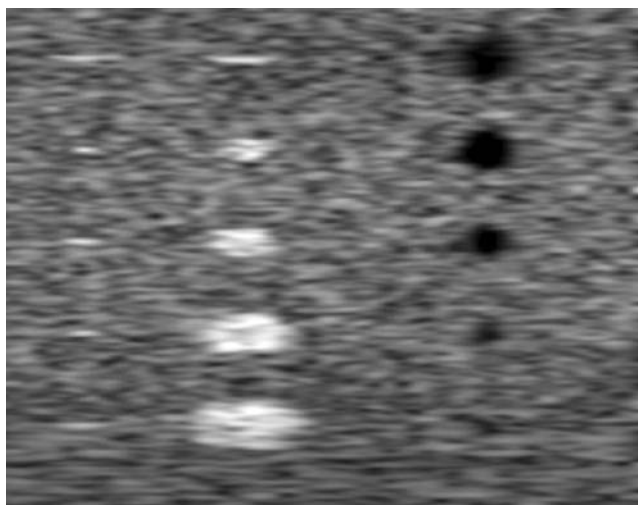


(b) Deformed image

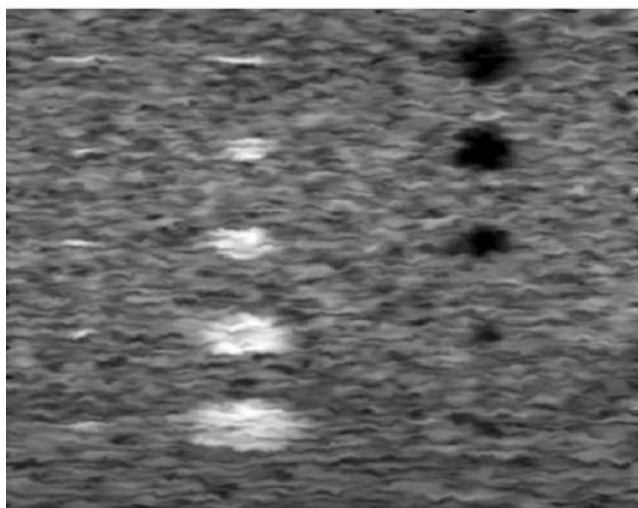
**Figure 2** a The first synthetic image and b its deformed image.

scattering regions with SNR 40 dB, followed by adding artificial speckle noise. Then, these two synthetic images are deformed by randomly generated displacement fields as shown in Figs. 2b and 3b, respectively. Our goal is to evaluate registration accuracy under non-rigid deformation. The displacement vectors that incur deformations are generated by random fields with pixel difference of 15 and 30 followed by Gaussian smoothing with  $\sigma = 6$  and  $\sigma = 15$  in Figs. 2b and 3b, respectively.

Experimental results with these two synthetic examples are shown in Table 1, where  $w$  and  $w'$  denote the ground truth displacement vector and the computed one using different methods, respectively. The mean ( $\mu_{w-w'}$ ) and the standard deviation ( $\sigma_{w-w'}$ ) of the error and the mean of the Sum of Squared Differences (SSD) between target and registered images are used as quantitative performance metrics. Three methods using



(a) Example 2



(b) Deformed image

**Figure 3** **a** The second synthetic image and **b** its deformed image.

different features are compared in Table 1. First, we only use the intensity term [15]; namely,

$$\int_{\Omega} \Psi(|S_I(\mathbf{x} + w(\mathbf{x})) - T_I(\mathbf{x})|^2) d\mathbf{x},$$

**Table 1** Comparison of three different data terms (unit:pixel).

Method		$I$	$I + G$	Proposed
Example1	$\mu_{w-w'}$	0.648	0.657	0.602
	$\sigma_{w-w'}$	0.995	0.918	0.850
	SSD	201.028	203.943	190.403
Example2	$\mu_{w-w'}$	4.150	4.015	3.776
	$\sigma_{w-w'}$	6.747	6.606	6.773
	SSD	23.183	22.731	21.719

in the data term, which denoted by  $I$  in Table 1. Next, both the intensity and its gradient features [8] are used in the data term. Mathematically, we have

$$\int_{\Omega} \Psi(|S_I(\mathbf{x} + w(\mathbf{x})) - T_I(\mathbf{x})|^2) + \gamma (|\nabla S_I(\mathbf{x} + w(\mathbf{x})) - \nabla T_I(\mathbf{x})|^2) d\mathbf{x},$$

which is denoted by  $I + G$  in the table. The third one is the proposed method that uses both the intensity and the local phase information. As to the smoothness term, the first two methods adopt the same one as the proposed method. We see from Table 1 the proposed method has a smaller registration error in terms of the mean and the standard deviation as well as smaller mean SSD than the other two methods.

We can adjust the importance of the data term and the smoothness term by tuning parameter  $\alpha$ . Likewise, by choosing  $\gamma$ , we can adjust the importance between different data term including an intensity, gradient and local phase term. We find the parameter values heuristically which minimize the energy functional most.

### 5.2 In Vivo Image

Furthermore, we use the *in vivo* cardiac ultrasound images of mice and human subjects for performance comparison. Gaussian smoothing is first performed on these ultrasound images as a pre-processing step since the intensity and its gradient can be sensitive to noise, resulting in undesired matching. The smoothed source and the target ultrasound images of mice and human subject are shown in Figs. 4 and 5a and b along with their intensity difference in Fig. 4 and 5c. For visual evaluation of the proposed algorithm, the difference image between the target and the registered images is presented in Figs. 4 and 5d and the displacement vector from the source image and the deformation field are presented in e and f, respectively.

As shown in the obtained deformation fields, the proposed method is able to find the displacement of pixels in the dark region that has similar intensity levels. Since there is no ground truth in the *in vivo* data, we compare registration accuracy using various similarity measures such as the mean SSD, the Mutual Information (MI) and the Normalized Correlation (NC) in Table 3. Since we used the L1 norm which is similar to the mean SSD, comparison using more generic metrics such as MI and NC demonstrates the validity of the

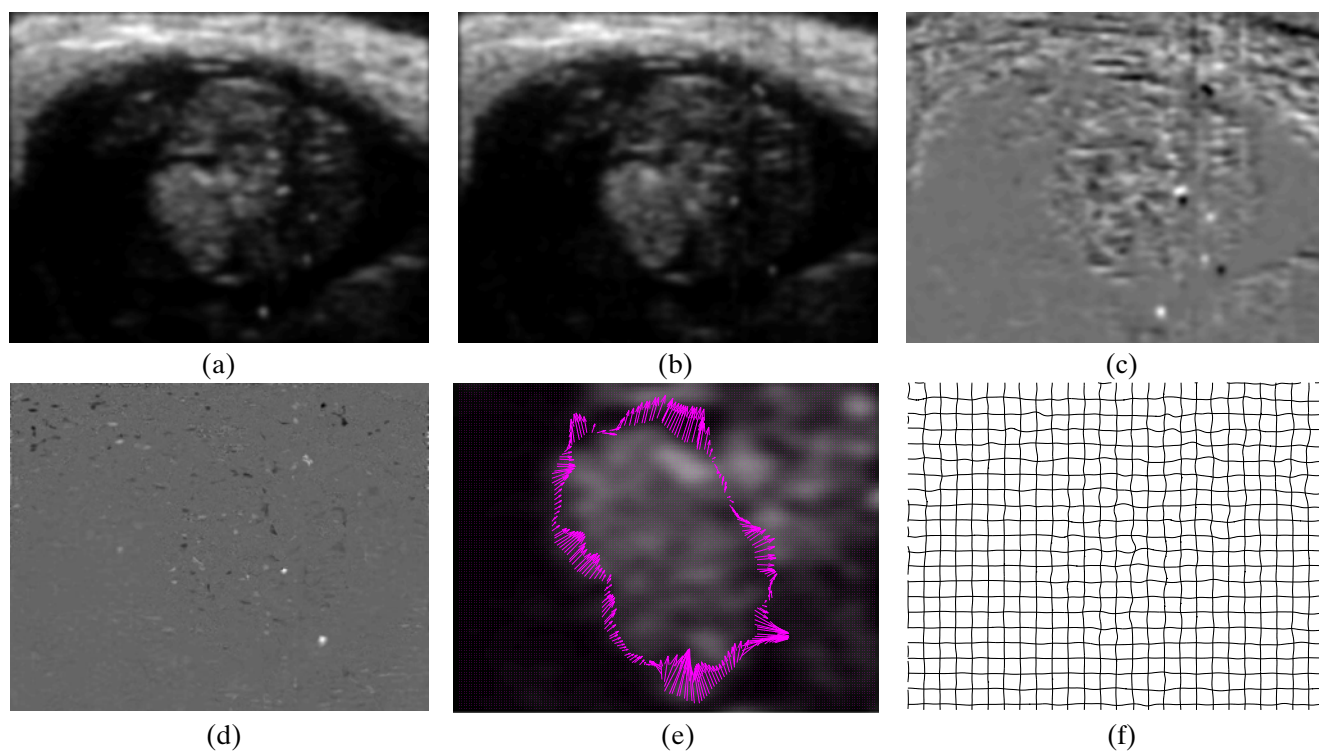


**Figure 4** *In vivo* mice ultrasound images: **a** the source image, **b** the target image, **c** the difference image between source and target images, **d** results obtained by the proposed method, **e** the

displacement vector from the boundary in **a** (arrows being scaled 1.5 times for the visualization purpose), and **f** the deformation field.

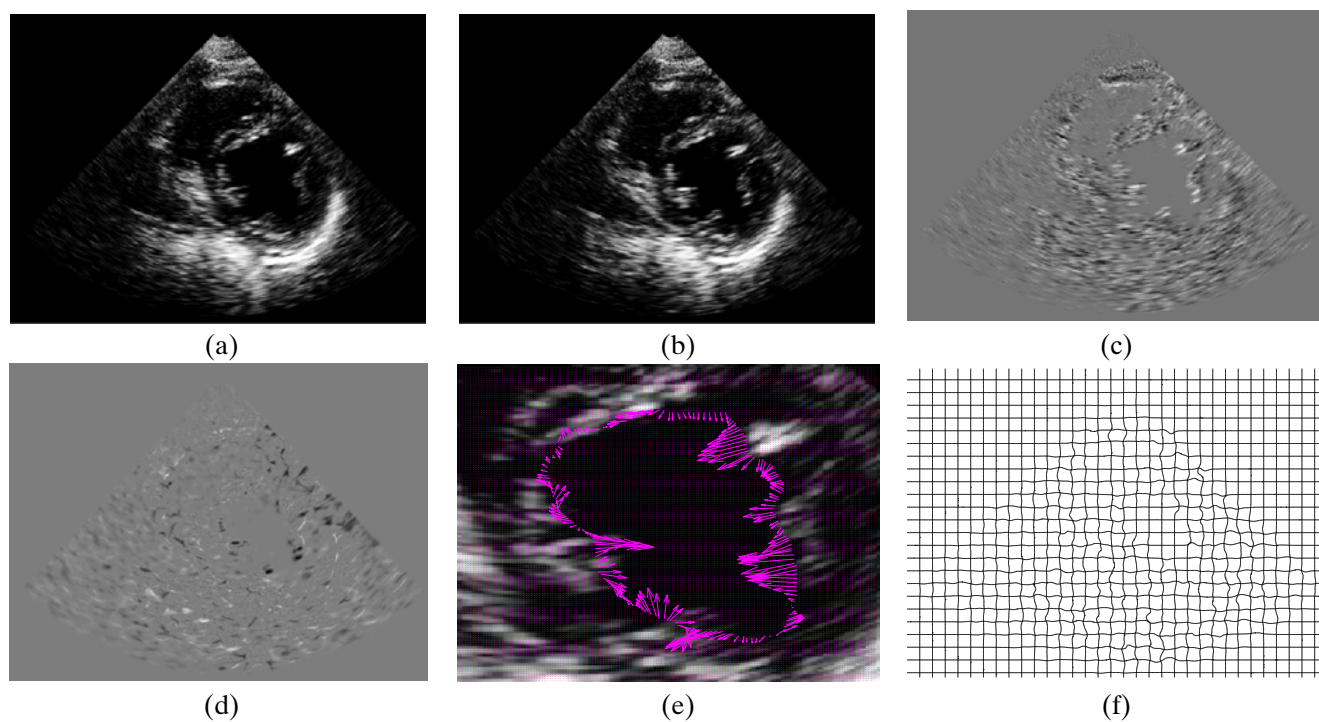


**Figure 5** *In vivo* human subject ultrasound images: **a** the source image, **b** the target image, **c** the difference image between source and target images, **d** results obtained by the proposed method, **e** the

displacement vector from the myocardium boundary in **a** (arrows being scaled 1.5 times for the visualization purpose), and **f** the deformation field.

**Table 2** Comparison of three different similarity measures for the mice image registration (in the unit of pixels).

Method		$I$	$I + G$	Proposed
Mice data	SSD	26.145	25.99	25.885
	MI	1.182	1.182	1.183
	NC	0.995	0.995	0.996

mean SSD as a similarity measure in ultrasound image registration (Table 2).

We see that there is a general trend between mean SSD, MI and NC in Table 3. That is, when SSD is lower, both MI and NC become higher. This demonstrates the usefulness of the similarity measure (*i.e.*, the mean SSD) as well as the energy functional.

## 6 Conclusion

We presented a novel non-rigid registration method for ultrasound images in this work. Specifically, we proposed to use the local phase function as a geometric feature to find correspondences of pixels in two ultrasound images that suffer from speckle, artifact and occlusion. By combining both the local phase and the intensity information under a variational framework, the proposed method outperforms others using the intensity and its gradient. Different similarity measures, including mean SSD, NC and MI, were used to compare the performance of different algorithms. Clinically, the proposed method can be applied to the analysis of tissue mechanic properties and object motion (e.g. beating heart) for the treatment of the myocardial perfusion and other diseases. In the future, we would like to extend this method so as to find motion of tissues in multiple frames, which is similar to optical flow and other vision related problems such as motion segmentation and tracking. Also the local phase can be used for velocity estimation or other tracking purposes as well.

**Table 3** Comparison of three different similarity measures for the human subject image registration (in the unit of pixels).

Method		$I$	$I + G$	Proposed
Human data	SSD	37.377	37.126	34.768
	MI	1.203	1.21	1.221
	NC	0.957	0.959	0.963

## References

- Shung, K. K., Smith, M. B., & Tsui, B. M. W. (1992). *Principles of medical imaging*. San Diego, CA: Academic.
- Shung, K. K. (2005). *Diagnostic ultrasound: Imaging and blood flow measurements*. Boca Raton, FL: Francis Taylor.
- Nelson, T. R., Downay, D. B., Pretorius, D. H., & Fenster, A. (1990). *Three-dimensional ultrasound*. Philadelphia, PA: Lippincott Williams & Wilkins.
- Picard, M., Popp, R., & Weyman, A. (2002). Assessment of left ventricular function by echocardiography: A technique in evolution. *Journal of the American Society of Echocardiography*, 21(3), 14–21.
- Ledesma-Carbayo, M. J., Kybic, J., Desco, M., et al. (2005). Spatio-temporal nonrigid registration for ultrasound cardiac motion estimation. *IEEE Transactions on Medical Imaging*, 24(9), 1113–1126 (September).
- Krucker, J., LeCarpentier, G., Fowlkes, J., & Carson, P. (2000). 3D spatial compounding of ultrasound images using image-based nonrigid registration. *Ultrasound in Medicine & Biology*, 26(9), 1475–1488.
- Slomka, P. J. (2004). Software approach to merging molecular with anatomic information. *Journal of Nuclear Medicine*, 45(1), 36–45.
- Brox, T., Bruhn, A., Papenberg, N., & Weickert, J. (2004). High accuracy optical flow estimation based on a theory for warping. In *European conference on computer vision, Prague, Czech Republic. LNCS* (Vol. 3024, pp. 25–36). Berlin: Springer (May).
- Bruhn, A., Weickert, J., Feddern, C., Kohlberger, T., & Schnorr, C. (2005). Variational optical flow computation in real time. *IEEE Transactions on Image Processing*, 14, 608–615.
- Mellor, M. (2004). *Phase methods for non-rigid medical image registration*. Ph.D. thesis, Oxford University.
- Makela, T., Clarysse, P., Sipila, O., Pauna, N., Pham, Q.C., Katila, T., et al. (2002). A review of cardiac image registration methods. *IEEE Transactions on Medical Imaging*, 21(9), 1011–1021.
- Giachetti, A. (1998). On-line analysis of echocardiographic image sequences. *Medical Image Analysis*, 2(3), 261–284.
- Chalana, V., Linker, D., Haynor, D., & Kim, Y. (1996). A multiple active contour model for cardiac boundary detection on echocardiographic sequences. *IEEE Transactions on Medical Imaging*, 15(3), 290–298.
- Herlin, I., & Ayache, N. (1992). Features extraction and analysis methods for sequences of ultrasound images. *Image and Vision Computing*, 10(10), 673–682.
- Zikic, D., Wein, W., Khamene, A., Clevert, D., & Navab, N. (2006). Fast deformable registration of 3d-ultrasound data using a variational approach. In *MICCAI. LNCS* (Vol. 3216, pp. 915–923). Berlin: Springer.
- Foroughi, P., & Abolmaesumi, P. (2005). Elastic registration of 3d ultrasound images. In *MICCAI. LNCS* (Vol. 3749, pp. 83–90). Berlin: Springer.
- Rohr, K., Spengel, H. S., et al. (2001). Landmark-based elastic registration using approximating thin-plate splines. *IEEE Transactions on Medical Imaging*, 20(6), 526–534.
- Morrone, M. C., & Owens, R. A. (1987). Feature detection from local energy. *Pattern Recognition Letters*, 6(5), 303–313.
- Mulet-Parada, M., & Noble, A. (1998). 2d+t acoustic boundary detection in echocardiography. In *MICCAI. LNCS* (Vol. 1496, pp. 806–813). Berlin: Springer.

20. Mellor, M., & Brady, M. (2005). Non-rigid multimodal image registration using local phase. In *MICCAI. LNCS* (Vol. 3216, pp. 789–796). Berlin: Springer.
21. Grau, V., Becher, H., & Noble, J. A. (2006). Phase-based registration of multi-view real-time three-dimensional echocardiographic sequences. In *MICCAI. LNCS* (pp. 612–619). Berlin: Springer.
22. Boukerroui, D., Noble, A., & Brady, M. (2004). On the choice of band-pass quadrature filters. *Journal of Mathematical Imaging and Vision*, 21(1), 53–80.
23. Felsberg, M., & Sommer, G. (2000). A new extension of linear signal processing for estimating local properties and detecting features. In *DAGM*, (pp. 195–202).
24. Horn, B., & Schunck, B. (1981). Determining optical flow. *Artificial Intelligence*, 17, 185–203.



**Jonghye Woo** received the B.S. degree from Seoul National University, Seoul, Korea, in 2005 and the M.S. degree from University of Southern California in 2007, all in Electrical Engineering. From 2002 to 2004, he served as a Korea Overseas Volunteer at Kutai Government, Indonesia. Currently he is a Ph.D. student in the Department of Electrical Engineering, University of Southern California and a visiting researcher in Artificial Intelligent in Medicine Program at Cedars-Sinai Medical Center. His research interests are in the areas of medical image analysis and computer vision. This includes image segmentation, registration and object tracking in various imaging modalities.



**Byung-Woo Hong** joined the School of Computer Science and Engineering at Chung-Ang University in Seoul, Korea as a faculty member in 2008 after his post-doctoral research at University of California Los Angeles since 2005. He obtained his Ph.D.

from University of Oxford in 2005, his master's from Weizmann Institute of Science in 1999, and his undergraduate from Chung-Ang University in 1995. His research interests include Computer Vision, Medical Image Analysis, and Image Processing.



**Changhong Hu** received his B.S. degree in Biomedical Engineering from Xi'an Jiaotong University in 1995, Xi'an, Shannxi, P.R. China, M.S. in Bioengineering from the Pennsylvania State University, University Park, PA, in 2002, and Ph.D. degree in Biomedical Engineering from University of Southern California, Los Angeles, in 2005. He is currently a Research Associate in Biomedical Engineering Department, University of Southern California. He is working on the development of high-frequency ultrasound imaging systems/electronics and digital signal processing. Mr. Hu is a member of the Institute of Electrical and Electronics Engineers (IEEE).



**K. Kirk Shung** obtained a B.S. in electrical engineering from Cheng-Kung University in Taiwan in 1968, a M.S. in electrical engineering from University of Missouri, Columbia, MO in 1970 and a Ph.D. in electrical engineering from University of Washington, Seattle, WA, in 1975. He did postdoctoral research at Providence Medical Center in Seattle, WA, for one year before being appointed a research bioengineer holding a joint appointment at the Institute of Applied Physiology and medicine. He became an assistant professor at the Bioengineering Program, Pennsylvania State University, University Park, PA in 1979 was promoted to professor in 1989. He was a Distinguished Professor of Bioengineering at Penn State until September 1, 2002 when he joined the Department of Biomedical Engineering, University of Southern California, Los Angeles, CA, as a professor. He

has been the director of NIH Resource on Medical Ultrasonic Transducer Technology since 1997.

Dr. Shung is a fellow of the IEEE, the Acoustical Society of America and the American Institute of Ultrasound in Medicine. He is a founding fellow of the American Institute of Medical and Biological Engineering. He has served for two terms as a member of the NIH Diagnostic Radiology Study Section. He received the IEEE Engineering in Medicine and Biology Society early career award in 1985 and was the coauthor of a paper that received the best paper award for IEEE Transactions on Ultrasonics, Ferroelectrics and Frequency Control (UFFC) in 2000. He was the distinguished lecturer for the IEEE UFFC society for 2002-2003. He was elected an outstanding alumnus of Cheng-Kung University in Taiwan in 2001.

Dr. Shung has published more than 200 papers and book chapters. He is the author of a textbook "Principles of Medical Imaging" published by Academic Press in 1992 and a text book "Diagnostic Ultrasound: Imaging and Blood Flow Measurements" published by CRC press in 2005. He co-edited a book "Ultrasonic Scattering by Biological Tissues" published by CRC Press in 1993. Dr. Shung's research interest is in ultrasonic transducers, high frequency ultrasonic imaging, and ultrasonic scattering in tissues.



**C.-C. Jay Kuo** received the B.S. degree from the National Taiwan University, Taipei, in 1980 and the M.S. and Ph.D. degrees from the Massachusetts Institute of Technology, Cambridge, in 1985 and 1987, respectively, all in Electrical Engineering. He is presently Director of the Signal and Image Processing Institute (SIPI) and Professor of Electrical Engineering, Computer Science and Mathematics at the University of Southern California (USC). His research interests are in the areas of digital image/video analysis and modeling, multimedia data compression, communication and networking, and biological signal/image processing. Dr. Kuo has guided 87 students to their Ph.D. degrees and supervised 20 postdoctoral research fellows. Currently, his research group at USC has around 35 Ph.D. students (please visit website <http://viola.usc.edu>), which is one of the largest academic research groups in multimedia technologies. He is co-author of about 145 journal papers, 745 conference papers and 9 books. He delivered about 350 invited lectures in conferences, research institutes, universities and companies.

Dr. Kuo is a Fellow of IEEE and SPIE. He received the National Science Foundation Young Investigator Award (NYI) and Presidential Faculty Fellow (PFF) Award in 1992 and 1993, respectively. He received the Northrop Junior Faculty Research Award from the USC Viterbi School of Engineering in 1994. He received the best paper awards from the multimedia communication Technical Committee of the IEEE Communication Society

in 2005, from the IEEE Vehicular Technology Fall Conference (VTC-Fall) in 2006, and from IEEE Conference on Intelligent Information Hiding and Multimedia Signal Processing (IIH-MSP) in 2006. He was an IEEE Signal Processing Society Distinguished Lecturer in 2006, and a recipient of the Okawa Foundation Research Grant in 2007. He is also Advisor to the SMPTE (Society of Motion Picture Television Engineers)-USC student chapter.



**Piotr Slomka** is currently a Research Scientist at Cedars-Sinai Medical Center in Los Angeles and Associate Professor of Medicine at the UCLA School of Medicine, positions he has held since 2002. He is also a Fellow of the American College of Cardiology and Fellow of the Canadian College of Physicists in Medicine. Prior to his current positions, he served as Assistant Professor in the Departments of Diagnostic Radiology, Nuclear Medicine and Medical Biophysics at the University of Western Ontario and as an Associate Scientist at the Robarts Research Institute in London, Ontario.

Dr. Slomka is widely recognized as one of the leading contributors in the world to the area of research in software algorithms for medical image analysis. His current focus is in the development of automated computer algorithms for myocardial perfusion quantification and multimodality image registration.

He received his Masters Degree in Medical Instrumentation from Warsaw University of Technology in Warsaw, Poland in 1989 and his PhD in Medical Biophysics from the University of Western Ontario, London, Ontario, Canada in 1995.

Most of Dr. Slomka's research accomplishments are in the field of automating visual interpretation of cardiac images and computer-aided detection of disease and combining multimodality data. In addition to his manuscript contributions, the results of his research have led to the development of several software packages for practical clinical imaging work that are used throughout the world.

Dr. Slomka was recently elected to be a Fellow of the American College of Cardiology. He has also been a Fellow of the Canadian College of Physicists in Medicine since 1997. He continues to serve as a reviewer for several leading journals, including the Journal of Nuclear Medicine, IEEE Transactions on Medical Imaging and Nuclear Science, the Journal of Nuclear Cardiology and the Journal of the American College of Cardiology. His teaching achievements in cardiology are recognized as well, as he repeatedly serves as invited faculty for major national and international cardiac imaging congresses.

He has co-authored over 79 peer-reviewed manuscripts, 8 book chapters and 102 peerreviewed abstracts. In the majority of his research work, he has been the principal scientific developer of the computer software applied to analysis of cardiac images.